HHS Public Access

Author manuscript

Liver Int. Author manuscript; available in PMC 2017 May 01.

Published in final edited form as:

Liver Int. 2016 May ; 36(5): 659–666. doi:10.1111/liv.13058.

Prospective comparison of magnetic resonance imaging to transient elastography and serum markers for liver fibrosis detection

Hadrien A. Dyvorne, PhD[1], **Guido H. Jajamovich, PhD**[1], **Octavia Bane, PhD**[1], **M. Isabel Fiel, MD**[2], **Hsin Chou, MS**[3], **Thomas D. Schiano, MD**[3], **Douglas Dieterich, MD**[3], **James S. Babb, PhD**[4], **Scott L. Friedman, MD**[3], and **Bachir Taouli, MD**[1,5]

[1]Translational and Molecular Imaging Institute, Icahn School of Medicine at Mount Sinai, New York, One Gustave Levy Place, Box 1234, New York, NY 10029 USA

[2]Department of Pathology, Icahn School of Medicine at Mount Sinai, New York, One Gustave Levy Place, Box 1234, New York, NY 10029 USA

[3]Department of Medicine, Division of Liver Diseases, Icahn School of Medicine at Mount Sinai, New York, One Gustave Levy Place, Box 1234, New York, NY 10029 USA

[4]Department of Radiology, New York University Langone Medical Center, New York, NY

[5]Department of Radiology, Icahn School of Medicine at Mount Sinai, New York, One Gustave Levy Place, Box 1234, New York, NY 10029 USA

Abstract

Background & Aims—Establishing accurate non-invasive methods of liver fibrosis quantification remains a major unmet need. Here, we assessed the diagnostic value of a multiparametric magnetic resonance imaging (MRI) protocol including diffusion-weighted imaging (DWI), dynamic contrast-enhanced (DCE)-MRI and magnetic resonance elastography (MRE) in comparison with transient elastography (TE) and blood tests [including ELF (Enhanced Liver Fibrosis) and APRI] for liver fibrosis detection.

Methods—In this single center cross-sectional study, we prospectively enrolled 60 subjects with liver disease who underwent multiparametric MRI (DWI, DCE-MRI and MRE), TE and blood tests. Correlation was assessed between non-invasive modalities and histopathologic findings including stage, grade, and collagen content, while accounting for covariates such as age, sex, BMI, HCV status and MRI-derived fat and iron content. ROC curve analysis evaluated the performance of each technique for detection of moderate-to-advanced liver fibrosis (F2–F4) and advanced fibrosis (F3–F4).

Results—MRE provided the strongest correlation with fibrosis stage ($r=0.66$, $p<0.001$), inflammation grade ($r=0.52$, $p<0.001$) and collagen content ($r=0.53$, $p=0.036$). For detection of

Correspondence: Bachir Taouli, MD, Icahn School of Medicine at Mount Sinai, Department of Radiology and Translational and Molecular Imaging Institute, 1470 Madison Ave, New York, NY 10029, USA, bachir.taouli@mountsinai.org, Tel: + 1 212 824-8453. SLF and BT: Co-last authors

Conflict of interest: None

moderate-to-advanced fibrosis (F2–F4), AUCs were 0.78, 0.82, 0.72, 0.79, 0.71 for MRE, TE, DCE-MRI, DWI, APRI, respectively. For detection of advanced fibrosis (F3–F4), AUCs were 0.94, 0.77, 0.79, 0.79, 0.70, respectively.

Conclusions—MRE provides the highest correlation with histopathologic markers and yields high diagnostic performance for detection of advanced liver fibrosis and cirrhosis, compared to DWI, DCE-MRI, TE and serum markers.

Keywords

liver fibrosis; magnetic resonance imaging; elastography; DWI; dynamic contrast-enhanced MRI

INTRODUCTION

Several non-invasive modalities, including transient elastography (TE), magnetic resonance imaging (MRI) and serum markers (1–4) have been proposed for liver fibrosis detection in hopes of decreasing the need for liver biopsy. Large cohort studies showed high performance for detection of fibrosis and cirrhosis using TE (5–7). Magnetic resonance elastography (MRE) is an emerging technique that estimates tissue stiffness distribution using MRI-based wave imaging in the liver. Recent MRE studies also reported high performance for liver fibrosis detection (8–16), although published data are smaller than those of TE. Diffusion-weighted MRI (DWI) probes molecular diffusion properties of tissues, and has shown changes with fibrosis stage, with restricted diffusion occurring in the presence of fibrosis (9, 17, 18). Intravoxel incoherent motion DWI is an advanced diffusion technique that attempts to separately assess perfusion and molecular diffusion components in tissues, with promising results for fibrosis and cirrhosis detection (19–22). Dynamic contrast-enhanced (DCE)-MRI can quantify hepatic perfusion changes that occur in advanced fibrosis and cirrhosis (20, 23, 24).

Despite the variety of potential non-invasive methods for fibrosis detection, only a small number of studies have compared different non-invasive methods (6, 8, 9, 18, 25). Wang et al (9) showed higher performance of MRE compared to DWI. In Patel et al (20), a higher detection performance was observed using DCE-MRI compared to DWI. Two studies (8, 14) have demonstrated superiority of MRE compared to TE or shear wave elastography (8, 14, 16), while another study found no difference (15). To date, no single study has performed a head-to-head comparison of multiparametric MRI with TE and serum markers.

In this initial cross-sectional study, we have prospectively evaluated the performance of MRI (including DWI, DCE-MRI and MRE) compared to TE and serum markers for liver fibrosis detection.

SUBJECTS AND METHODS

Subjects

This was a HIPAA compliant single tertiary care center prospective cross-sectional study, funded by the National Institutes of Health and approved by Mount Sinai IRB. All subjects gave informed consent prior to the study. 60 subjects with liver disease (M/F 40/20, mean

age 55 y, range 23–69 y) were enrolled between October 2010 and June 2014 (Table 1). Twelve healthy volunteers (M/F 8/4, mean age 29 y, age range 19–42 y) were recruited via clinicaltrials.gov (#NCT01600105) in order to perform protocol optimization and to evaluate test-retest reproducibility. Patients were recruited from the Division of Liver Diseases or from the Surgical Oncology Clinic at Mount Sinai. 48 patients had liver fibrosis assessed by liver biopsy (mean delay between biopsy and MRI: 85 d, range 21–201 d), 9 subjects had hepatocellular carcinoma with liver fibrosis assessed on hepatectomy specimens, and one patient underwent liver transplantation for cirrhosis. Two patients with cirrhosis are listed for liver transplantation (Child Pugh class A: n=1, and B: n=1). Etiologies of liver disease were chronic hepatitis C virus (HCV) infection [n=49, including 3 with concomitant NASH, 1 with associated alcohol intoxication, 1 with concomitant primary biliary cirrhosis (PBC), 1 with chronic hepatitis B virus (HBV) co-infection], NASH (n=7), chronic HBV (n=2), PBC (n=1), and autoimmune hepatitis (n=1). Patients with renal insufficiency (eGFR <30, n=10) did not undergo DCE-MRI but were enrolled for the other modalities. All subjects were asked to fast for 6 hours before the study.

MRI acquisition and processing (See supplemental document/supplemental Table 1)

From October 2010 to May 2013, subjects were scanned on 1.5T (Magnetom Avanto & Aera, Siemens) and 3.0T (GE750, GE Healthcare) systems equipped with multichannel spine and body coil arrays. From May 2013 to June 2014, patients underwent DCE and IVIM DWI examination on a 1.5T system. MRE was acquired on the 3.0T system where the MRE hardware was installed. 1.5T systems were used in order to reduce the effect of distortion on DWI series compared to 3.0T (26). Subjects were positioned arms up in a supine position. Although multiple platforms were used, we and others have showed recently (27–30) that the variability of quantitative metrics across platforms is of the same order or lower than inter-scan variability.

Image analysis was performed by imaging scientists who applied the relevant signal modeling to region of interests placed in the liver tissue (DCE-MRI: GHJ, postdoc with 2 years experience; IVIM and MRE: HAD, postdoc with 3 years experience; and fat & iron quantification: OB, postdoc with 2 years experience). Hepatic fat and iron content were assessed at 1.5T (supplemental Table 1).

Intravoxel incoherent motion DWI (n=60): was performed using a single shot echo planar imaging sequence with fat suppression, sampling 16 b values (0, 15, 30, 45, 60, 75, 90, 105, 120, 135, 150, 175, 200, 400, 600 and 800 s/mm^2) to separate perfusion from diffusion effects in the diffusion decay.

DCE-MRI (n=51)—T1-weighted DCE-MRI was acquired using a 3D-FLASH sequence before and after the injection of gadolinium contrast (0.05 mmol/Kg of gadobenate dimeglumine, Multihance, Bracco Diagnostics) followed by a 25 ml saline flush only in patients with estimated GFR > 60 mL/min/1.73m^2. DCE-MRI was not performed in 9 patients with renal insufficiency. Because of the high relaxivity of Multihance, only half dose was injected to decrease saturation effects at high concentrations (31).

MRE (n=41)—A passive acoustic driver (Resoundant, Rochester, USA) placed against the right anterior chest wall with its center level with the xiphoid process was used to generate mechanical waves in the liver at a frequency of 60 Hz. Wave imaging was performed using a fast gradient echo based multislice 2D MRE sequence. MRE equipment was made available at our institution starting from March 2012, thus only 42 of 60 subjects underwent MRE exam.

TE (n=48)—TE (FibroScan, Echosens, France) was performed on the same day as the MRI exam by three operators, using a 3.5 MHz probe in intercostal approach and 50 Hz transient waves. The value retained for liver stiffness (in kPa) was the median of 10 successful measures, with interquartile range lower than 30%.

Serum markers (n=54)—Blood samples were drawn the same day as the MRI exam for the Enhanced Liver Fibrosis test (ELF™, Siemens Healthcare, Tarrytown, NY, USA) (3, 4) as well as to determine the AST to platelet ratio (APRI). Blood tests were not available in 6 patients who declined the blood testing.

Histopathologic evaluation

Histopathologic assessment was performed by an experienced pathologist. Liver specimens consisting of core needle biopsies (measuring at least 15 mm in length and containing at least 5 portal tracts) and large tissue sections from resection specimens were assessed. The liver specimens were formalin-fixed and paraffin-embedded and stained with hematoxylin-eosin staining for routine morphologic analysis and for quantification of steatosis. Slides stained with Perls' Prussian blue for identification of hemosiderin deposition and Masson trichrome stain for assessment of degree of fibrosis were also utilized. The METAVIR (in HCV/HBV) or the Brunt (in NASH) semiquantitative scoring systems (32, 33) were used for histopathologic determination of the stage of fibrosis and grade of inflammation (fibrosis stage: F0–F4, activity grade: A0–A3). Collagen content was also quantified (see supplemental document).

Statistical analyses

Age, gender, BMI, HCV status, fat and iron content were assessed as potential confounding factors by testing their association with the METAVIR stage and grade using Spearman correlations (for age and BMI) and exact Mann-Whitney tests (for gender, HCV status, presence of iron or fat). Spearman rank correlation coefficients were used to characterize the association of non-invasive measures with histopathologic measures with confounding factors included as covariates. Logistic regression was used to test the utility of the measures for the detection of moderate-to-advanced fibrosis (F2–F4) and advanced fibrosis (F3–F4) and to elect combinations of non-invasive parameters providing improved detection. To control for varying sample size (n), we used precision (1/n) as a weighting factor in the analysis, penalizing modalities with higher sample size to offset the greater power their larger sample size affords. ROC analysis was performed to characterize the detection performance of single non-invasive parameters. AUCs were compared between techniques using the Delong test. Manual calculations of sensitivity and specificity were performed for combinations of two or more parameters with AUC ≥0.70. For combinations of parameters,

the diagnosis of fibrosis was considered positive if at least n-1 of n parameters gave positive diagnosis (e.g. for combinations of 2 parameters, diagnosis is positive if at least 1 parameter gives positive diagnosis).

RESULTS

Patient population (Table 1)

Cirrhotic pre-transplant patients without histopathology (n=2) were assigned stage 4, but were not assigned an activity score. Based on MRI findings, 22 patients had steatosis [grade 1 (up to 33%, n=18), grade 2 (33–66%, n=3) and grade 3 (>66%, n=1)], and 11 had iron deposition (mild, n=8, and moderate, n=3). Collagen quantification was technically feasible in 51 patients, with range of Sirius index of 0.2–42.4%.

Failure rate—DWI and MRE failed in 3/60 (5.0%) and 4/41 (9.7%) patients, respectively; in relation with hepatic iron deposition (n=3 for DWI and MRE), and mechanical failure of MRE system (n=1). DCE-MRI failed in 1/51 (1.9%) patients. TE failed in 2/48 (4.1%) subjects due to the presence of ascites or overweight.

Parameter reproducibility results are reported in the supplemental document.

Correlation with fibrosis stage, inflammation grade and collagen content

There was no significant correlation of age with either grade (p=0.39) or stage (p=0.49), or of BMI with grade (p=0.177) or stage (p=0.27). There was a significant gender difference in terms of stage (p <0.001), but not of grade (p=0.835). Stage (p=0.24) and grade (p=0.155) were not significantly different according to HCV status. Stage and grade were also not significantly different between patients with fat (p= 0.17/0.95) or iron (p=0.84/0.1) deposition. The potential confounding effects of age, gender, BMI, HCV, fat and iron, were accounted for by conducting analyses with these factors included as covariates. Significant correlations were observed between non-invasive techniques and fibrosis stage/inflammation grade (Table 2). The strongest correlation was observed between MRE and fibrosis stage (r=0.66, p <0.001). Liver stiffness measured with MRE was the only metric that correlated significantly with collagen content (r=0.53, p=0.036). True diffusion coefficient (D) measured with DWI, mean transit time (MTT) and time to peak (TTP) measured with DCE-MRI and liver stiffness measured with TE also correlated significantly with stage and/or stage. There was no significant correlation between ELF score and stage/grade, while APRI correlated with both grade and stage.

Detection of moderate-to-advanced fibrosis (F2–F4) (Fig. 1–2, Table 3)

MRE was the only significant predictor of moderate-to-advanced fibrosis (p=0.027). However, the AUC of MRE was not significantly different from that of other modalities (p >0.31). Among serum markers, ELF (p=0.434) was not a statistically significant predictor of fibrosis, while APRI (p=0.076) showed a trend of increasing values with advanced fibrosis.

Detection of advanced fibrosis (F3–F4) (Table 3)

Mean transit time measured with DCE-MRI, liver stiffness measured with TE and APRI were all significant predictors of advanced fibrosis, while trends were observed for true diffusion coefficient (D) and liver stiffness measured with MRE, likely due to sample size. The best detection performance was achieved by MRE, which was significantly better than that of DWI ($p < 0.001$) and DCE-MRI (TTP, $p = 0.01$). However, the AUC of MRE was not significantly different than that of the other modalities ($p > 0.062$). ELF was not a statistically significant predictor of advanced fibrosis ($p = 0.134$). Of note, ELF test had a low diagnostic performance with AUCs of 0.61 and 0.63, respectively for F2–F4 and F3–F4.

Combination of non-invasive metrics

The analysis did not identify any set of two or more imaging measures representing significant independent predictors of fibrosis (see also supplemental document for manual calculations of sensitivity and specificity for association of different parameters).

DISCUSSION

In this initial study, we have evaluated the diagnostic performance of advanced MRI methods compared to TE and serum markers for detection of liver fibrosis in patients with chronic liver disease. While almost all modalities correlated with histopathologic findings, MRE had the strongest correlation with fibrosis stage and collagen content, and the highest performance for detection of advanced fibrosis, while its performance was equivalent to that of TE and other MRI modalities for detection of moderate-to-advanced fibrosis.

In the fibrotic liver, collagen deposition tends to restrict water diffusion leading to a decrease in true and apparent diffusion coefficients. Previous studies using ADC (which includes diffusion and perfusion contributions) have shown to reflect changes with fibrosis (9, 17, 18). Beyond ADC measurement, multiple b-values acquisition may be applied to estimate also tissue perfusion, with encouraging results for liver fibrosis and cirrhosis (19, 20, 22, 34). Yoon et al (21) observed good performance for fibrosis detection using pseudodiffusion and ADC. In our experience, the true diffusion coefficient yielded similar performance compared to ADC, although demonstrating better correlation with stage and grade; while perfusion fraction and pseudodiffusion coefficient did not correlate with degree of fibrosis, as opposed to prior studies (19, 20, 22).

With DCE-MRI, perfusion properties of the liver can be measured using a paramagnetic contrast agent, leading to parenchymal flow estimates that may be used as markers of hemodynamic changes in cirrhosis and portal hypertension. With increasing fibrosis, higher resistance to flow and compartmentalization develops in liver parenchyma, which should lead to increased tracer transit time. DCE-MRI parameters were shown previously to predict the presence of advanced liver fibrosis and cirrhosis (20, 23, 24). In our study, the best detection performance was observed with mean transit time for advanced fibrosis. Unlike previous reports (20, 23, 24), the arterial buffer response was not observed with higher fibrosis stages in our study. Although mean transit time shows similar performance as TE for

advanced fibrosis detection, it should be mentioned that DCE-MRI cannot be performed in subjects with renal failure, and requires more complex processing.

TE has been investigated in large cohorts for fibrosis and cirrhosis detection (6, 7, 15, 16, 35, 36). We observed good detection performance for F2–F4 and F3–F4 detection, with AUCs slightly lower than what was previously reported. Proposed thresholds for F3–F4 detection in previous reports (6, 7, 18, 35) range from 9.5 – 12.9 kPa, while we found an optimal threshold of 8.6 kPa. Our threshold of 6.8 kPa for detection of F2–F4 fibrosis was in the lower range of published thresholds (6.5–8.9 kPa) (14, 15). Liver stiffness values obtained from MRE and TE are supposed to be proportional, with a stiffness value 2.5–3 fold higher for TE (14, 37).

MRE has been compared to DWI (9) and TE (8, 14, 15) in previous studies. We found that MRE provided the highest performance for advanced fibrosis detection, with AUC as high as 0.94, in agreement with previous reports (8–10, 14, 15). For moderate-to-advanced fibrosis detection, we observed lower AUC compared to prior studies (8, 10). Our optimal threshold for F3–F4 detection was 4.07 kPa compared to 3.13–6.47 kPa (for F3–F4) (8–10). This variability is likely due to different MRE implementations, platform differences and patient population studied.

The correlation between TE and collagen content has been previously reported (38, 39) ($r=0.59–0.64$, $p<0.001$). There is little data on the correlation between MRI techniques and collagen content. A recent study (12) in chronic HBV showed a strong correlation between MRE and morphometric quantification of fibrosis ($r=0.78$), higher than what we observed. Of note, the methods of collagen quantification used are not equivalent. It remains to be seen if changes in stiffness can be detected prospectively to assess the effect of antiviral or antifibrotic therapy.

MRE exam is fast, and the implementation and post-processing are relatively simple. In addition, the multi-parametric nature of MRI allows for a more complete assessment of organ structure and function (hepatic fat and iron content, DWI and contrast-enhanced sequences for HCC detection). Because of its high reproducibility, MRE may also be a better candidate than TE to assess response to antiviral or antifibrotic therapy. However, the disadvantage of MRE is the requirement for hardware and software additions to the MRI platform, which may not be available in all centers, and higher cost.

Some parameters that correlated with fibrosis stage also showed some significant correlation with inflammation grade (true diffusion coefficient, mean transit time, and liver stiffness measured with TE and MRE), which may be of value for detection of inflammation in NASH (13, 40). Inflammation might also be considered a confounding factor for fibrosis detection (41), and future studies should investigate the effect of inflammation in a larger cohort of patients. Other factors such as iron and fat content may also alter quantitative parameters. For this reason, we accounted for the effect of fat or iron by including them as covariates in the analysis. Iron deposition contributed to measurement failure for DWI and MRE in 3 patients.

There are notable limitations to our study. First, the sample size is small, reflecting our initial training set, and thus the findings need to be validated in an independent cohort. Second, there was a difference in sample size between techniques, due to availability, failure rate, and exclusion criteria. Third, different platforms were used for MRI, which could lead to variability in the findings. However, recent studies have reported inter-platform variability of the same order as or lower than inter-scan variability (27–30).

In conclusion, our results show that MRE is the most accurate non-invasive technique for advanced fibrosis detection compared to DWI, DCE-MRI, TE and blood tests; while MRE had equivalent performance to TE and DWI for detection of moderate-to-advanced fibrosis (F2–F4) in patients with chronic liver disease.

Supplementary Material

Refer to Web version on PubMed Central for supplementary material.

Acknowledgments

Funding: NIH Grant 1R01DK087877; GE Healthcare; Siemens USA (Both GE Healthcare and Siemens AG had no control on the data) NIH DK56621, NIH AA020709

We would like to thank Richard L. Ehman, MD for research support and guidance.

List of Abbreviations (in alphabetical order)

ADC	apparent diffusion coefficient
APRI	AST to Platelet Ratio Index
CV	coefficient of variation
D	true diffusion coefficient
D*	pseudodiffusion coefficient
DWI	diffusion-weighted imaging
DCE-MRI	dynamic contrast-enhanced MRI
DV	distribution volume
ELF	enhanced liver fibrosis
Fa	arterial flow
Fp	portal flow
Ft	total hepatic flow
FLASH	Fast Low Angle Shot
FOV	field of view
LS	liver stiffness
MRI	magnetic resonance imaging

MRE	magnetic resonance elastography
MTT	mean transit time
PF	perfusion fraction
PV	portal venous fraction
ROI	region of interest
TE	transient elastography
TTP	time to peak

References

1. WAI CT, GREENSON JK, FONTANA RJ, KALBFLEISCH JD, MARRERO JA, CONJEEVARAM HS, et al. A simple noninvasive index can predict both significant fibrosis and cirrhosis in patients with chronic hepatitis C. Hepatology. 2003; 38(2):518–26. [PubMed: 12883497]
2. POYNARD T, IMBERT-BISMUT F, MUNTEANU M, MESSOUS D, MYERS RP, THABUT D, et al. Overview of the diagnostic value of biochemical markers of liver fibrosis (FibroTest, HCV FibroSure) and necrosis (ActiTest) in patients with chronic hepatitis C. Comp Hepatol. 2004; 3(1):8. [PubMed: 15387887]
3. ROSENBERG WM, VOELKER M, THIEL R, BECKA M, BURT A, SCHUPPAN D, et al. Serum markers detect the presence of liver fibrosis: a cohort study. Gastroenterology. 2004; 127(6):1704–13. [PubMed: 15578508]
4. MAYO MJ, PARKES J, ADAMS-HUET B, COMBES B, MILLS AS, MARKIN RS, et al. Prediction of clinical outcomes in primary biliary cirrhosis by serum enhanced liver fibrosis assay. Hepatology. 2008; 48(5):1549–57. [PubMed: 18846542]
5. ZIOL M, HANDRA-LUCA A, KETTANEH A, CHRISTIDIS C, MAL F, KAZEMI F, et al. Noninvasive assessment of liver fibrosis by measurement of stiffness in patients with chronic hepatitis C. Hepatology. 2005; 41(1):48–54. [PubMed: 15690481]
6. CASTERA L, VERGNIOL J, FOUCHER J, LE BAIL B, CHANTELOUP E, HAASER M, et al. Prospective comparison of transient elastography, Fibrotest, APRI, and liver biopsy for the assessment of fibrosis in chronic hepatitis C. Gastroenterology. 2005; 128(2):343–50. [PubMed: 15685546]
7. FOUCHER J, CHANTELOUP E, VERGNIOL J, CASTERA L, LE BAIL B, ADHOUTE X, et al. Diagnosis of cirrhosis by transient elastography (FibroScan): a prospective study. Gut. 2006; 55(3): 403–8. [PubMed: 16020491]
8. HUWART L, SEMPOUX C, VICAUT E, SALAMEH N, ANNET L, DANSE E, et al. Magnetic resonance elastography for the noninvasive staging of liver fibrosis. Gastroenterology. 2008; 135(1): 32–40. [PubMed: 18471441]
9. WANG Y, GANGER DR, LEVITSKY J, STERNICK LA, MCCARTHY RJ, CHEN ZE, et al. Assessment of chronic hepatitis and fibrosis: comparison of MR elastography and diffusion-weighted imaging. AJR Am J Roentgenol. 2011; 196(3):553–61. [PubMed: 21343496]
10. YIN M, TALWALKAR JA, GLASER KJ, MANDUCA A, GRIMM RC, ROSSMAN PJ, et al. Assessment of hepatic fibrosis with magnetic resonance elastography. Clin Gastroenterol Hepatol. 2007; 5(10):1207–13. e2. [PubMed: 17916548]
11. ZHAO JD, LIU J, REN ZG, GU K, ZHOU ZH, LI WT, et al. Maintenance of Sorafenib following combined therapy of three-dimensional conformal radiation therapy/intensity-modulated radiation therapy and transcatheter arterial chemoembolization in patients with locally advanced hepatocellular carcinoma: a phase I/II study. Radiat Oncol. 2010; 5:12. [PubMed: 20149262]
12. VENKATESH SK, XU S, TAI D, YU H, WEE A. Correlation of MR elastography with morphometric quantification of liver fibrosis (Fibro-C-Index) in chronic hepatitis B. Magn Reson Med. 2014; 72(4):1123–9. [PubMed: 24166665]

13. LOOMBA R, WOLFSON T, ANG B, BOOKER J, BEHLING C, PETERSON M, et al. Magnetic resonance elastography predicts advanced fibrosis in patients with nonalcoholic fatty liver disease: A prospective study. Hepatology. 2014
14. WU WP, CHOU CT, CHEN RC, LEE CW, LEE KW, WU HK. Non-Invasive Evaluation of Hepatic Fibrosis: The Diagnostic Performance of Magnetic Resonance Elastography in Patients with Viral Hepatitis B or C. PLoS One. 2015; 10(10):e0140068. [PubMed: 26469342]
15. BOHTE AE, DE NIET A, JANSEN L, BIPAT S, NEDERVEEN AJ, VERHEIJ J, et al. Non-invasive evaluation of liver fibrosis: a comparison of ultrasound-based transient elastography and MR elastography in patients with viral hepatitis B and C. Eur Radiol. 2014; 24(3):638–48. [PubMed: 24158528]
16. YOON JH, LEE JM, JOO I, LEE ES, SOHN JY, JANG SK, et al. Hepatic fibrosis: prospective comparison of MR elastography and US shear-wave elastography for evaluation. Radiology. 2014; 273(3):772–82. [PubMed: 25007047]
17. TAOULI B, TOLIA AJ, LOSADA M, BABB JS, CHAN ES, BANNAN MA, et al. Diffusion-weighted MRI for quantification of liver fibrosis: preliminary experience. AJR Am J Roentgenol. 2007; 189(4):799–806. [PubMed: 17885048]
18. LEWIN M, POUJOL-ROBERT A, BOELLE PY, WENDUM D, LASNIER E, VIALLON M, et al. Diffusion-weighted magnetic resonance imaging for the assessment of fibrosis in chronic hepatitis C. Hepatology. 2007; 46(3):658–65. [PubMed: 17663420]
19. LUCIANI A, VIGNAUD A, CAVET M, NHIEU JT, MALLAT A, RUEL L, et al. Liver cirrhosis: intravoxel incoherent motion MR imaging--pilot study. Radiology. 2008; 249(3):891–9. [PubMed: 19011186]
20. PATEL J, SIGMUND EE, RUSINEK H, OEI M, BABB JS, TAOULI B. Diagnosis of cirrhosis with intravoxel incoherent motion diffusion MRI and dynamic contrast-enhanced MRI alone and in combination: preliminary experience. J Magn Reson Imaging. 2010; 31(3):589–600. [PubMed: 20187201]
21. YOON JH, LEE JM, BAEK JH, SHIN CI, KIEFER B, HAN JK, et al. Evaluation of hepatic fibrosis using intravoxel incoherent motion in diffusion-weighted liver MRI. J Comput Assist Tomogr. 2014; 38(1):110–6. [PubMed: 24378888]
22. MURPHY P, HOOKER J, ANG B, WOLFSON T, GAMST A, BYDDER M, et al. Associations between histologic features of nonalcoholic fatty liver disease (NAFLD) and quantitative diffusion-weighted MRI measurements in adults. J Magn Reson Imaging. 2014
23. VAN BEERS BE, MATERNE R, ANNET L, HERMOYE L, SEMPOUX C, PEETERS F, et al. Capillarization of the sinusoids in liver fibrosis: Noninvasive assessment with contrast-enhanced MRI in the rabbit. Magn Reson Med. 2003; 49(4):692–9. [PubMed: 12652540]
24. HAGIWARA M, RUSINEK H, LEE VS, LOSADA M, BANNAN MA, KRINSKY GA, et al. Advanced liver fibrosis: diagnosis with 3D whole-liver perfusion MR imaging--initial experience. Radiology. 2008; 246(3):926–34. [PubMed: 18195377]
25. ZHAO H, CHEN J, MEIXNER DD, XIE H, SHAMDASANI V, ZHOU S, et al. Noninvasive assessment of liver fibrosis using ultrasound-based shear wave measurement and comparison to magnetic resonance elastography. J Ultrasound Med. 2014; 33(9):1597–604. [PubMed: 25154941]
26. ROSENKRANTZ AB, OEI M, BABB JS, NIVER BE, TAOULI B. Diffusion-weighted imaging of the abdomen at 3.0 Tesla: image quality and apparent diffusion coefficient reproducibility compared with 1.5 Tesla. J Magn Reson Imaging. 2011; 33(1):128–35. [PubMed: 21182130]
27. CUI Y, DYVORNE H, BESA C, COOPER N, TAOULI B. IVIM Diffusion-weighted Imaging of the Liver at 3.0T: Comparison with 1.5T. European J Radiol Open. 2015; 2:123–28. [PubMed: 26393236]
28. DONATI OF, CHONG D, NANZ D, BOSS A, FROEHLICH JM, ANDRES E, et al. Diffusion-weighted MR imaging of upper abdominal organs: field strength and intervendor variability of apparent diffusion coefficients. Radiology. 2014; 270(2):454–63. [PubMed: 24471390]
29. SERAI SD, YIN M, WANG H, EHMAN RL, PODBERESKY DJ. Cross-vendor validation of liver magnetic resonance elastography. Abdom Imaging. 2015; 40(4):789–94. [PubMed: 25476489]

30. YASAR TK, WAGNER M, BANE O, BESA C, BABB JS, KANNENGIESSER S, et al. Interplatform reproducibility of liver and spleen stiffness measured with MR elastography. J Magn Reson Imaging. 2015

31. SCHABEL MC, PARKER DL. Uncertainty and bias in contrast concentration measurements using spoiled gradient echo pulse sequences. Phys Med Biol. 2008; 53(9):2345–73. [PubMed: 18421121]

32. BEDOSSA P, POYNARD T. An algorithm for the grading of activity in chronic hepatitis C. The METAVIR Cooperative Study Group. Hepatology. 1996; 24(2):289–93. [PubMed: 8690394]

33. BRUNT EM, JANNEY CG, BISCEGLIE AMD, NEUSCHWANDER-TETRI BA, BACON BR. Nonalcoholic steatohepatitis: a proposal for grading and staging the histological lesions. The American Journal of Gastroenterology. 1999; 94(9):2467–74. [PubMed: 10484010]

34. DYVORNE HA, GALEA N, NEVERS T, FIEL MI, CARPENTER D, WONG E, et al. Diffusion-weighted imaging of the liver with multiple b values: effect of diffusion gradient polarity and breathing acquisition on image quality and intravoxel incoherent motion parameters--a pilot study. Radiology. 2013; 266(3):920–9. [PubMed: 23220895]

35. FRIEDRICH-RUST M, WUNDER K, KRIENER S, SOTOUDEH F, RICHTER S, BOJUNGA J, et al. Liver fibrosis in viral hepatitis: noninvasive assessment with acoustic radiation force impulse imaging versus transient elastography. Radiology. 2009; 252(2):595–604. [PubMed: 19703889]

36. LUCIDARME D, FOUCHER J, LE BAIL B, VERGNIOL J, CASTERA L, DUBURQUE C, et al. Factors of accuracy of transient elastography (fibroscan) for the diagnosis of liver fibrosis in chronic hepatitis C. Hepatology. 2009; 49(4):1083–9. [PubMed: 19140221]

37. OUDRY J, CHEN J, GLASER KJ, MIETTE V, SANDRIN L, EHMAN RL. Cross-validation of magnetic resonance elastography and ultrasound-based transient elastography: a preliminary phantom study. J Magn Reson Imaging. 2009; 30(5):1145–50. [PubMed: 19856447]

38. ZIOL M, KETTANEH A, GANNE-CARRIE N, BARGET N, TENGHER-BARNA I, BEAUGRAND M. Relationships between fibrosis amounts assessed by morphometry and liver stiffness measurements in chronic hepatitis or steatohepatitis. Eur J Gastroenterol Hepatol. 2009; 21(11):1261–8. [PubMed: 19478678]

39. ISGRO G, CALVARUSO V, ANDREANA L, LUONG TV, GARCOVICH M, MANOUSOU P, et al. The relationship between transient elastography and histological collagen proportionate area for assessing fibrosis in chronic viral hepatitis. J Gastroenterol. 2012

40. CHEN J, TALWALKAR JA, YIN M, GLASER KJ, SANDERSON SO, EHMAN RL. Early detection of nonalcoholic steatohepatitis in patients with nonalcoholic fatty liver disease by using MR elastography. Radiology. 2011; 259(3):749–56. [PubMed: 21460032]

41. SHI Y, GUO Q, XIA F, DZYUBAK B, GLASER KJ, LI Q, et al. MR Elastography for the Assessment of Hepatic Fibrosis in Patients with Chronic Hepatitis B Infection: Does Histologic Necroinflammation Influence the Measurement of Hepatic Stiffness? Radiology. 2014; 273(1):88–98. [PubMed: 24893048]

Key points

1. MRE provides the highest correlation with fibrosis stage, inflammation grade and collagen content compared to DWI, DCE-MRI, TE and blood tests.
2. MRE yields high diagnostic performance for the detection of F3–F4 fibrosis, higher than that of any other non-invasive technique.
3. For detection of F2–F4 fibrosis, MRE had equivalent performance to TE.
4. Multiparametric analysis did not reveal independent predictors of liver fibrosis among non-invasive modalities, suggesting that fibrosis detection might be better achieved with a single modality such as MRE.

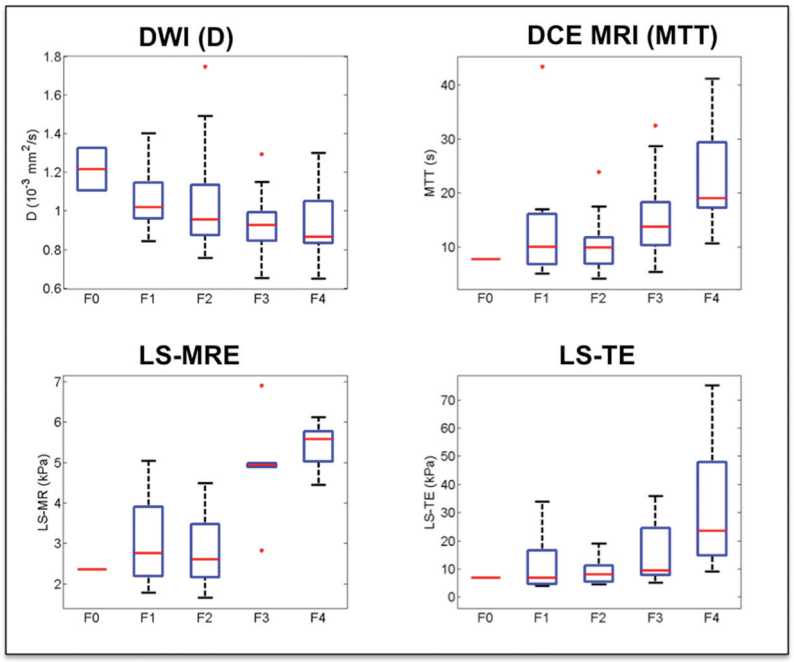

Fig. 1.

Distribution of select non-invasive parameters according to liver fibrosis stage. With increasing fibrosis stage, true diffusion coefficient (D) decreased; while liver mean transit time (MTT), liver stiffness measured with magnetic resonance elastography (LS-MRE) and liver stiffness measured with TE (LS-TE) increased.

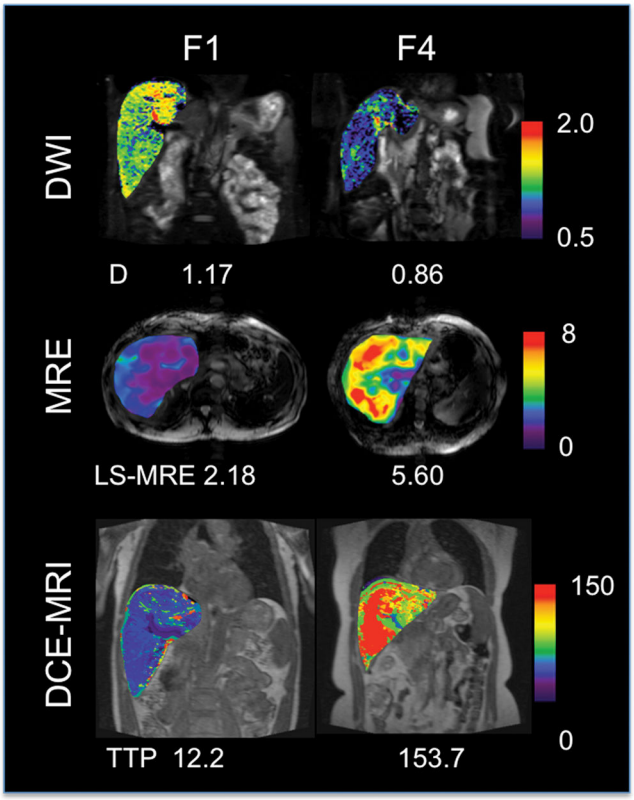

Fig. 2.

Parametric maps of true diffusion coefficient (D, in $x10^{-3}$ mm^2/s) measured with intravoxel incoherent motion DWI, shear liver stiffness measured with MRE (LS-MRE, in kPa); and time to peak (TTP, in sec) measured with DCE-MRI for two representative patients with fibrosis stage F1 (male, 51 y) and F4 (female, 65 y). There is lower diffusion coefficient, higher stiffness and longer time to peak in the cirrhotic patient (parameter values are listed on the image). Transient liver stiffness measured with TE was 4.4 (F1) and 25.1 kPa (F4).

Table 1

Characteristics of population studied.

Parameter	N=60
Sex (M/F)	40/20
Age (y)	55.2 ± 10 (23–69)
BMI (kg/m^2)	26.7 ± 4.4 (18.2–36.8)
Etiology of liver disease (n=60)	
HCV	49 (81.6%)
Non-HCV	11 (18.4%)
Histologic activity (METAVIR)	
A0	6
A1	21
A2	23
A3	8
Fibrosis score	
F0	2
F1	10
F2	21
F3	16
F4	11 *
Sirius index **	10.2 ± 9.1% (0.2–42.4%)

* Includes 2 cirrhotic patients listed for liver transplant

** n=51

Table 2

Spearman correlation (r) and corresponding p values for the association of non-invasive metrics with fibrosis stage, inflammation grade and Sirius index. Only parameters with at least one significant correlation were presented (p values are bolded when significant).

Technique	Parameter measured	Stage		Grade		Sirius index	
		r	r	r	p	r	p
DWI	**D**	−0.29	0.072	−0.32	**0.041**	−0.10	0.627
DCE-MRI	**Ft**	−0.37	**0.031**	−0.28	0.099	−0.05	0.819
	MTT	0.54	**0.001**	0.52	**0.002**	0.06	0.793
MRE	**LS-MRE**	0.66	**<0.001**	0.58	**0.002**	0.53	**0.036**
TE	**LS-TE**	0.58	**0.001**	0.24	0.200	0.31	0.134
Blood tests	**APRI**	0.56	**0.001**	0.41	**0.015**	0.20	0.310

D: true diffusion coefficient, DCE-MRI: dynamic contrast enhanced MRI, APRI: AST to platelet ratio, Ft: total hepatic low, LS-MRE: shear liver stiffness measured with MRE, LS-TE: liver stiffness measured with TE, MTT: mean transit time, TE: transient elastography.

Table 3

Performance of non-invasive modalities for detection of F2–F4 and F3–F4 fibrosis. Parameter values are given as mean ± standard deviation. Only parameters with AUC ≥0.70 are displayed.

Technique	Parameter	F0–F1	F2–F4	p*	AUC	Threshold	Sensitivity	Specificity
DWI	**D**	1.08 ± 0.16	0.98 ± 0.20	0.158	0.79 (0.56–0.93)	<1.00	75 (48–92)	83 (36–100)
MRE	**LS-MRE**	2.95 ± 0.99	3.99 ± 1.49	**0.027**	0.78 (0.55–0.92)	>3.90	56 (30–80)	100 (54–100)
TE	**LS-TE**	11.07 ± 10.40	16.29 ± 15.25	0.252	0.82 (0.60–0.95)	>6.80	87 (62–98)	83 (36–100)
DCE-MRI	**MTT**	13.6 ± 11.9	15.6 ± 8.7	0.567	0.72 (0.48–0.89)	>16.9	44 (20–70)	100 (54–100)
Blood tests	**APRI**	0.44 ± 0.27	1.12 ± 1.22	0.076	0.70 (0.56–0.82)	>0.48	41 (26–58)	100 (71–100)
		F0–F2	**F3–F4**	**p***	**AUC**	**Threshold**	**Sensitivity**	**Specificity**
DWI	**D**	1.06 ±0.21	0.94 ± 0.16	0.061	0.79 (0.56–0.93)	<0.92	67 (30–92)	85 (55–98)
MRE	**LS-MRE**	2.88 ± 0.91	5.16 ± 0.95	0.062	0.94 (0.80–0.99)	>4.07	92 (64–100)	92 (73–99)
TE	**LS-TE**	9.55 ± 6.85	21.44 ± 17.86	**0.012**	0.77 (0.62–0.89)	>8.60	77 (55–92)	70 (47–87)
DCE-MRI	**MTT**	11.6 ± 8.1	18.8 ± 9.1	**0.01**	0.79 (0.65–0.89)	>11.5	80 (59–93)	72 (51–88)
Blood tests	**APRI**	0.68 ± 0.69	1.32 ± 1.41	**0.033**	0.71 (0.56–0.83)	>0.84	75 (53–90)	57 (37–75)

* p values from logistic regression analysis (bolded when significant, p <0.05).

95% confidence intervals are given in parenthesis for AUC, sensitivity and specificity.

DWI: diffusion-weighted imaging, D: true diffusion coefficient (10^{-3} mm^2/s), MRE: magnetic resonance elastography, TE: ultrasound TE, LS-MRE: shear liver stiffness (kPa) measured with MRE, LS-TE: transient liver stiffness (kPa), DCE-MRI: dynamic contrast-enhanced magnetic resonance imaging, MTT: mean transit time, APRI: AST to Platelet Ratio Index